AD-A266 642

AlGaAs Diode Laser Blue Shift Resulting from Fast Neutron Irradiation

Prepared by

J. C. CAMPARO, S. B. DELCAMP, and R. P. FRUEHOLZ
Electronics Technology Center
Technology Operations

10 November 1992

Prepared for

**SPACE AND MISSILE SYSTEMS CENTER
AIR FORCE MATERIEL COMMAND**
Los Angeles Air Force Base
P. O. Box 92960
Los Angeles, CA 90009-2960

Engineering and Technology Group

THE AEROSPACE CORPORATION
El Segundo, California

93-15708

CYNTHIA B. TENEROWICZ, Lt., USAF
Program Manager
Advanced Comm Satellites

WM KYLE SNEDDON, Capt, USAF
Deputy Chief
Industrial & International Programs Division

REPORT DOCUMENTATION PAGE		
1a. REPORT SECURITY CLASSIFICATION Unclassified		**1b. RESTRICTIVE MARKINGS**
2a. SECURITY CLASSIFICATION AUTHORITY		**3. DISTRIBUTION/AVAILABILITY OF REPORT** Approved for public release; distribution unlimited
2b. DECLASSIFICATION/DOWNGRADING SCHEDULE		
4. PERFORMING ORGANIZATION REPORT NUMBER(S) TR-0091(6925-13)-2		**5. MONITORING ORGANIZATION REPORT NUMBER(S)** SMC-TR-93-27
6a. NAME OF PERFORMING ORGANIZATION The Aerospace Corporation Technology Operations	**6b. OFFICE SYMBOL** *(If applicable)*	**7a. NAME OF MONITORING ORGANIZATION** Space and Missile Systems Center
6c. ADDRESS *(City, State, and ZIP Code)* El Segundo, CA 90245-4691		**7b. ADDRESS** *(City, State, and ZIP Code)* Los Angeles Air Force Base Los Angeles, CA 90009-2960
8a. NAME OF FUNDING/SPONSORING ORGANIZATION	**8b. OFFICE SYMBOL** *(If applicable)*	**9. PROCUREMENT INSTRUMENT IDENTIFICATION NUMBER** F04701-88-C-0089
8c. ADDRESS *(City, State, and ZIP Code)*		**10. SOURCE OF FUNDING NUMBERS**

		PROGRAM ELEMENT NO.	PROJECT NO.	TASK NO.	WORK UNIT ACCESSION NO.

11. TITLE *(Include Security Classification)*

AlGaAs Diode Laser Blue Shift Resulting from Fast Neutron Irradiation

12. PERSONAL AUTHOR(S)
Camparo, James C.; Delcamp, Spencer B.; and Frueholz, Robert P.

13a. TYPE OF REPORT	**13b. TIME COVERED** FROM _____ TO _____	**14. DATE OF REPORT** *(Year, Month, Day)* 1992 November 10	**15. PAGE COUNT** 28

16. SUPPLEMENTARY NOTATION

17. COSATI CODES			**18. SUBJECT TERMS** *(Continue on reverse if necessary and identify by block number)*
FIELD	**GROUP**	**SUB-GROUP**	Lasers, Neutrons, Gain Curves

19. ABSTRACT *(Continue on reverse if necessary and identify by block number)*

Six TJS (transverse junction stripe) AlGaAs diode lasers were exposed to fast neutrons with fluences ranging from 2×10^{12} to 3×10^{13} n/cm^2, and their tuning, gain, and dispersion curves were measured. The tuning and gain curves of four lasers showed blue shifts of several meV at neutron fluences as low as 2×10^{12} n/cm^2; the other two lasers never showed this blue shift. In addition, the lasers that displayed a blue shift also showed an increase in their threshold currents. None of the lasers exhibited any change in their dispersion curves. To explain the blue shift, it is hypothesized that neutron irradiation reduces the efficiency for lasing in the bandtail states of these devices, forcing lasing action to occur between states with greater energy separation. A model in which the reduced efficiency takes the form of a decrease in the transition matrix element is found to yield blue shifts of the correct order of magnitude. Though bandtail effects may also explain the difference in radiation sensitivity among the TJS lasers, at present the reason why only four of the six lasers blue shifted after neutron irradiation is not well understood.

20. DISTRIBUTION/AVAILABILITY OF ABSTRACT [X] UNCLASSIFIED/UNLIMITED ☐ SAME AS RPT. ☐ DTIC USERS	**21. ABSTRACT SECURITY CLASSIFICATION** Unclassified
22a. NAME OF RESPONSIBLE INDIVIDUAL	**22b. TELEPHONE** *(Include Area Code)*	**22c. OFFICE SYMBOL**

DD FORM 1473, 84 MAR 83 APR edition may be used until exhausted. All other editions are obsolete.

PREFACE

Accesion For		
NTIS CRA&I		X
DTIC TAB		☐
Unannounced		☐
Justification		
By		
Distribution /		
Availability Codes		
Dist	Avail and / or Special	
A-1		

DTIC QUALITY INSPECTED 3

1

CONTENTS

FIGURES

I. INTRODUCTION

Many diode laser applications avail themselves of the device's brightness and bandwidth, and consequently there has been interest in how these laser properties are affected by a radiation environment. There are other applications however, that benefit more directly from the laser's spectral characteristics, in particular lasing wavelength tunability. For example, the next genera- tion of cesium and rubidium atomic clocks will employ diode lasers for optical pumping,[1] and this requires that the laser wavelength be tuned to within $\sim 2 \times 10^{-6}$ nm of an atomic resonance.[2] Therefore, in addition to brightness and bandwidth, there is a desire to understand how radiation environments can affect diode laser spectral characteristics. In the present work, this issue is con- sidered by examining the effect of fast neutrons on the lasing wavelengths of TJS (transverse junction stripe) AlGaAs diode lasers.

The effect of fast neutrons on the optical properties of GaAs has been a subject of serious study since the work of Aukerman *et al.*[3] in the early 1960s, and subsequent work has elaborated on their findings. In the regime of high neutron fluence, greater than $\sim 10^{17}$ n/cm^2, neutron exposure results in a marked increase in photon absorption at energies below the band-gap energy E_g. The absorption coefficient in this energy range increases like the square of the photon energy, and increases linearly with neutron fluence up to about 10^{18} n/cm^2 [4] McNichols and Ginell[5] have hypothesized that this behavior is due to photon absorption by $\sim 10 - 100$-nm-diam. metallic like regions resulting from the irradiation, and evidence in support of this hypothesis has been obtained by Tuomi and Tiainen.[6] Coates and Mitchell have seen similar absorption coeffi- cient behavior, and suggest that a ~ 5-nm-diam. region of high defect concentration exists in an extended spike of defects extending some tens of nanometers.[4] These authors argue that the defect regions are in the form of interstitial/vacancy pairs, and detailed calculations of neutron damage in GaAs would tend to support their conjecture.[7] For intermediate neutron fluences, in the vicinity of 10^{16} n/cm^2, neutron exposure still results in photon absorption at energies less than E_g, but in this regime the absorption coefficient increases exponentially with photon energy.[8] At low levels of neutron exposure, $\sim 10^{15} n$/cm^2 or less, there is no observable effect of fast neutrons on the absorption coefficient for energies less than E_g[9] and one might conclude that optical characteristics of GaAs devices are unaltered at these low fluence levels. Transport charac- teristics, however, are affected by these neutron fluences. After exposure to a neutron fluence of 10^{14} n/cm^2, Ludman and Nowak[10] obtained evidence of trapping states in GaAs with energies hundreds of meV below the conduction-band edge.

Though these studies of optical absorption are certainly relevant to laser operation, and similar behavior is expected for AlGaAs, there are considerations that mitigate against a simple extrapolation of these results to AlGaAs diode lasers. The absorption coefficient of a material only specifies the material's linear interaction with electromagnetic fields. Lasers, however, are nonlinear devices. More important, diode lasers are built from several layers of different band- gap materials, and are often highly doped. Both of these factors are known to influence degra- dation coefficients associated with neutron exposure.[11,12] Consequently, though there is no observable effect of fast neutrons on GaAs's optical-absorption coefficient at low fluence levels, it does not follow that AlGaAs diode lasers are unaffected by these same low levels of neutron exposure. For example, at $\sim 10^{13}$ n/cm^2 researchers have found in GaAs, AlGaAs ,and InGaAsP

5

diode lasers that threshold current is an increasing function of neutron fluence.[13,14] Barnes[15] has explained this phenomenon as due to an increase in nonradiative recombination in the laser's active region. Apparently, fast neutron irradiation creates both trapping sites and centers of nonradiative recombination in these materials. It is therefore plausible that low neutron exposure levels could affect the spectral characteristics of diode lasers, and in particular affect the lasing wavelength. To investigate this possibility, six lasers were exposed to fast neutron fluences ranging from 2×10^{12} to 3×10^{13} n/cm^2, and their gain curves, tuning curves, and dispersion curves were examined.

II. EXPERIMENT

The six diode lasers employed in this study comprised two different Mitsubishi TJS(transverse junction stripe) diode laser models: model 4102-01 and model 3101. (Details of device construction and geometry can be found in Ref. 30.) The 4102-01 diode lasers were labeled 4A-4D, and the 3101 diode lasers were labeled 3A and 3B. As indicated by the manufacturer's specified characteristics, which are collected in Table I, the two laser models differ in their threshold current and lasing wavelength. Since the 4102-01 diode lasers have a shorter emission wavelength, the mole fraction of Al in their active regions is larger than that of the 3101 diode lasers. In a manner to be discussed subsequently, we estimated the mole fraction of Al for the 4102-01 diode lasers as 0.13, and the mole fraction of Al for the 3101 diode lasers as 0.08. Both laser models are specified to emit a single longitudinal and transverse mode with an output power of several mW, and this was verified during preirradiation testing. After each irradiation, but prior to gain and tuning curve measurements, the diode lasers were subjected to a "burn-in." Burn-in consisted of operating the diode lasers for at least 8 h at current levels roughly 1.3 times the preirradiated threshold. Knowing the rate at which cw lasing wavelength changes with injection current, we estimated that during burn-in the 4102-01 diode lasers experienced a 30°C temperature rise above room temperature in their active regions, while the 3101 diode lasers only experienced an 8°C temperature rise. Both temperature increases, however, are well below expected annealing temperatures.[3] A seventh, control diode laser, was also subjected to testing, but was not irradiated. Constancy of the control laser's measured characteristics ensured that parameters associated with the experimental arrangement did not change appreciably over the ~one year of testing.

In order to measure the gain and tuning curves, the diode lasers were placed in a thermally stabilized mount (stability better than 0.1 °C), and the laser output was focused onto the entrance slits of a scanning monochromator. Wavelength resolution was measured to be 0.06 nm. The monochromator was calibrated using the known emission spectrum from a rubidium discharge lamp, and this calibration was checked following each neutron exposure. For the gain curve measurements, a linear polarizer was placed after the lens in order to eliminate the contribution of TM (transverse magnetic) modes to the laser's output spectrum.[16] For the tuning curve measurements, the linear polarizer was replaced by a 1.0 neutral density filter, which acted as a beam splitter. The diverted portion of the laser output was directed to a Fabr$_j$-Perot scanning interferometer with a 313 GHz free spectral range. For both the gain and tuning curve measurements, the light from the monochromator exit slit was made incident on an RCA 4832 GaAs photomultiplier tube (PMT), and care was taken to ensure that the PMT was not saturated. The PMT current was measured with a picoammeter and recorded on a strip chart as the monochromator grating rotated.

We employed Hakki and Paoli's technique for measuring diode laser gain,[17] where gain is related to the "visibility" of a laser's longitudinal cavity modes,

$$g(\lambda) = \frac{-\ln(R)}{L} - \frac{1}{L} \ln\left(\frac{\sqrt{r^+} + \sqrt{r^-}}{\sqrt{r^+} - \sqrt{r^-}}\right).$$ (1)

Table I. Nominal Characteristics of Diode Lasers Used in the Present Study as Specified by Manufacturer.

Laser	Model	Threshold Current[a] at 25°C (mA)	Lasing Wavelength at 25°C (nm)
3A	3101	12	816
3B	3101	12	818
4A	4102-01	34	783
4B	4102-01	36	785
4C	4102-01	33	784
4D	4102-01	35	784

[a]For the 4102-01 diode lasers, the typical device threshold current is specified as 30 mA by the manufacturer. For the 3101 diode lasers, the typical device threshold current is specified as 20 mA.

Here, $g(\lambda)$ is the laser gain at wavelength λ, R is the facet reflectivity, L is the laser cavity length, and we have assumed that the cavity filling factor is near unity. (In the present experiment we are only interested in relative changes of gain due to neutron exposure, so that the actual value of the cavity filling factor is not an issue.) I^+ and I^- correspond to maxima and minima, respectively, of the modal intensity spectrum emitted by the laser below threshold. The separation between successive maxima in this spectrum corresponds to the cavity mode spacing $|\Delta\lambda(\lambda)|$ at the maxima's average wavelength. Using this technique, gain curves were measured at both 15 and 30°C, for between five and eight different values of the injection current at each temperature. (Temperature here refers to the nominal temperature of the diode laser; no attempt was made to compensate for the effect of cw injection current heating.)

To employ Eq. (1) it is necessary to know both the facet reflectivity and the cavity length for each laser. In general, though, facet reflectivity only depends on the refractive index n of the semiconductor,[18]

$$R = (n-1)^2 / (n+1)^2 . \tag{2}$$

Hence, it was only necessary to know the index of refraction and cavity length of each laser. Since the laser basically corresponds to a Fabry-Perot cavity, the index of refraction and cavity length are related to each other through the cavity mode spacing,

$$L = \lambda^2 / \left[2n(\lambda)|\Delta\lambda(\lambda)|\right]. \tag{3}$$

Cavity lengths could therefore be determined prior to irradiation by ignoring dispersion (which is small), and by employing Eq. (3) with an average refractive index for each laser n_{avg} and an average cavity mode spacing. The average refractive index was evaluated by noting that the

nominal lasing wavelength λ_L is near the band-gap energy E_g, and that the band-gap energy is linearly related to the mole fraction x of Al in the active region,[19]

$$hc \, / \, \lambda_L \sim E_g(eV) = 1.424 + 1.247x$$

Once the approximate Al content of the preirradiated diode lasers was known, it was possible to use the data of Casey, Sell, and Panish[20] to estimate n_{avg}.

Since the low levels of neutron exposure employed in the present study could not have altered the physical lengths of the laser cavities by more than a few thousandths of a percent,[4] these lengths were treated as constants. After the preirradiation estimation of L, Eq. (3) was used to determine n (λ) from a measurement of the cavity mode spacings as a function of λ. In this manner we were able to investigate neutron-induced changes in the laser material's dispersion.

For the tuning curve measurements (lasing wavelength versus injection current), the scanning Fabry-Perot interferometer output was observed on an oscilloscope whose horizontal deflection was calibrated to the étalon's free spectral range. As the laser injection current was increased there was a corresponding shift of the lasing wavelength, and this could be measured by the horizontal displacement of the laser line on the oscilloscope. Laser mode hops could easily be discerned, since they appeared as a discontinuous change in the laser line's position on the oscilloscope, and after a mode hop an absolute wavelength determination was made with the monochromator. In this fashion tuning curves were recorded at both 15 and 30°C for each laser.

The lasers were irradiated with neutrons from the SPR-III pulsed reactor at Sandia National Laboratories. The pulse width [full width at half-maximum (FWHM)] for this reactor is 76 μs, and the neutron energy spectrum is similar to an unmoderated U^{235} fission spectrum.[21] Exposure occurred at room temperature, and the quoted fluence represents the average value of measurements from three sulfur dosimeters. Appropriate corrections were applied to the dosimeter values to convert them to fluences for neutrons with energies greater than 1 meV. No attempt was made to orient the lasers in any specific way for their exposure to neutrons.

III. RESULTS

A. TUNING

Figure 1 shows two representative diode laser tuning curves for various levels of neutron exposure. Prior to irradiation all lasers displayed the typical staircase like tuning curve,[22] with mode hops separated by regions of continuous single mode tuning, and we note that even after irradiation the slope of the continuous tuning regions was unchanged. However, though neither laser 3A nor 3B showed any appreciable change in the position of their tuning curves, lasers 4A–4D all showed similar displacements of their tuning curves to shorter wavelengths. (The slight variation in the positions of laser 3A's tuning curves are not indicative of neutron-induced effects; they reflect the limits of our ability to reset diode laser temperature in the ~2 months between each neutron exposure.) Furthermore, it should be mentioned that up to a neutron fluence of 3×10^{13} n/cm^2, lasers 3A and 3B showed no change in their threshold current. When lasers 4A–4D showed blue shifts, they also showed increases in their threshold currents and decreases in their CW differential external quantum efficiencies. Finally, though laser 4D showed mode hops to shorter, rather than longer wavelength after irradiation, this should not be taken as a necessary result of neutron exposure. Nonirradiated diode lasers have also shown this anomalous mode hopping behavior.[23]

There are several facts worth noting about the blue shift of the 4102-01 diode laser tuning curves. First of all, the blue shift, as well as the threshold current increase, was observed at a very low level of neutron exposure. Further, since the tuning curves are obtained for the laser operating above threshold, the blue shift is manifested in the nonlinear regime of field-matter interactions, and the shift has a magnitude of approximately 1 nm or several meV. The shift appears to saturate with neutron exposure, since there is no difference in the tuning curves of laser 4D for neutron exposures of 1×10^{13} and 3×10^{13} n/cm^2. Finally, the shift does not occur immediately on exposure to neutrons. The tuning curve of laser 4D after 2×10^{12} n/cm^2, but prior to burn-in, is similar to the preirradiation tuning curve. Only after laser 4D had been operating for several hours was there any noticeable change in the laser's tuning curve.

B. GAIN

Figure 2 illustrates the effect of fast neutrons on laser 4A's gain curves, and the solid lines are least-squares fits of the data to a fifth-order polynomial. For a given gain curve , the least-squares fit is used to find the photon energy corresponding to peak gain E_p and to find the photon energies where the gain is zero. On the gain curve's short-wavelength size, the photon energy corresponding to zero gain can be used as a measure of the energy separation between the conduction- and valence-band quasi-Fermi levels ΔF_{cv} (so long as the laser is well below threshold). Regarding laser 4A's gain curves, exposure to fast neutrons has caused the entire gain curve to shift to the blue. In particular, fast neutron exposure appears to have caused ΔF_{cv} to increase. The observation of the gain curve blue shift is consistent with the tuning curve results. However, since the laser is operating below threshold, the minority-carrier density in the active region is at a reduced level, and the observations are now in the regime of linear field-matter interactions, where the third-order susceptibility of the material is unimportant.
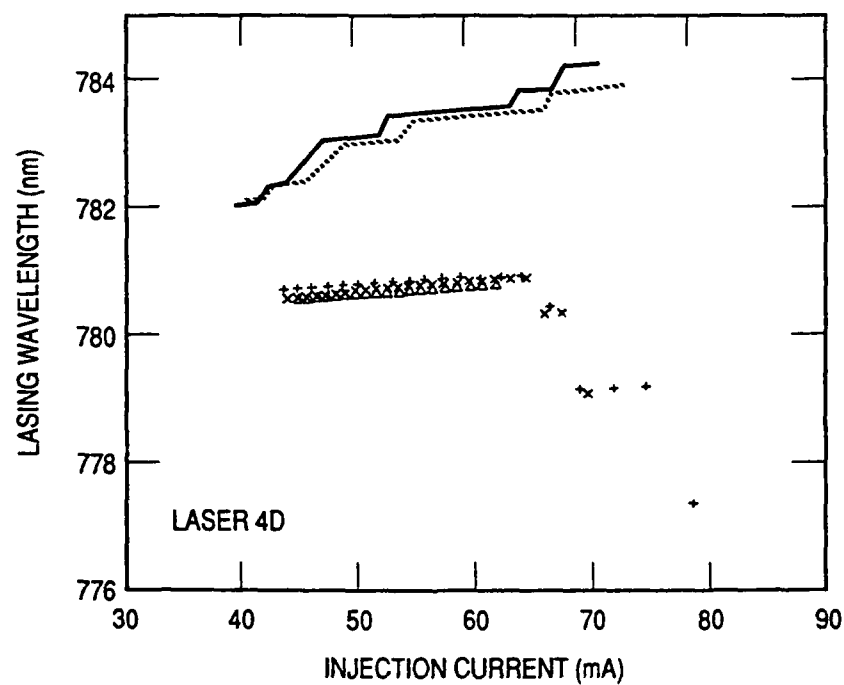
11
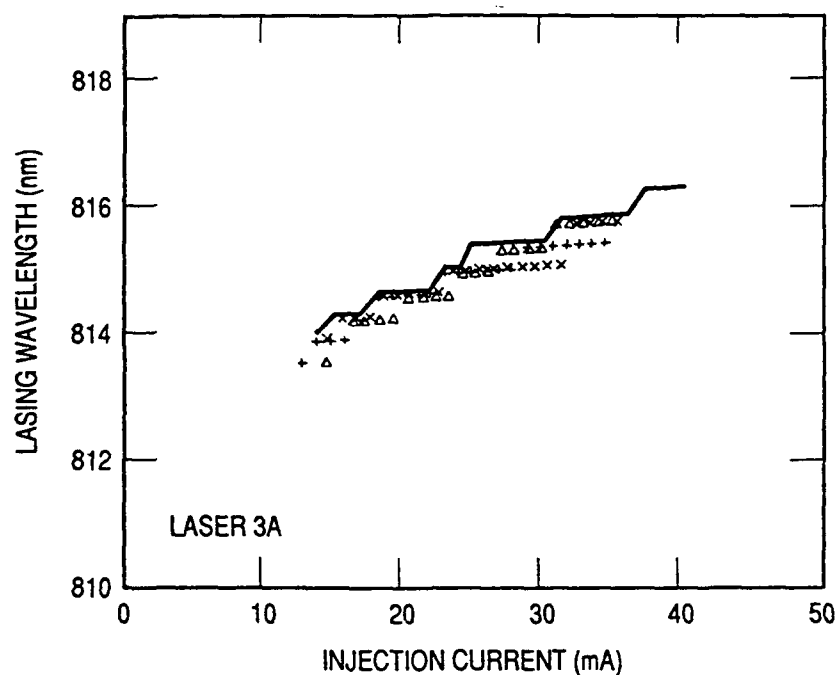
Figure 1. Tuning curves of two representative diode lasers at 15°C. Laser 3A was a model 3101 diode laser, and laser 4D was a model 4102-01 diode laser. The solid curves correspond to the preirradiation tuning curve results; crosses correspond to a fluence of 2×10^{12} n/cm^2; $\times$'s correspond to a fluence of 1×10^{13} n/cm^2, and triangles correspond to a fluence of 3×10^{13} n/cm^2. For laser 4D, the dashed line corresponds to the laser's tuning curve after exposure to 2×10^{13} n/cm^2, but prior to burn-in.
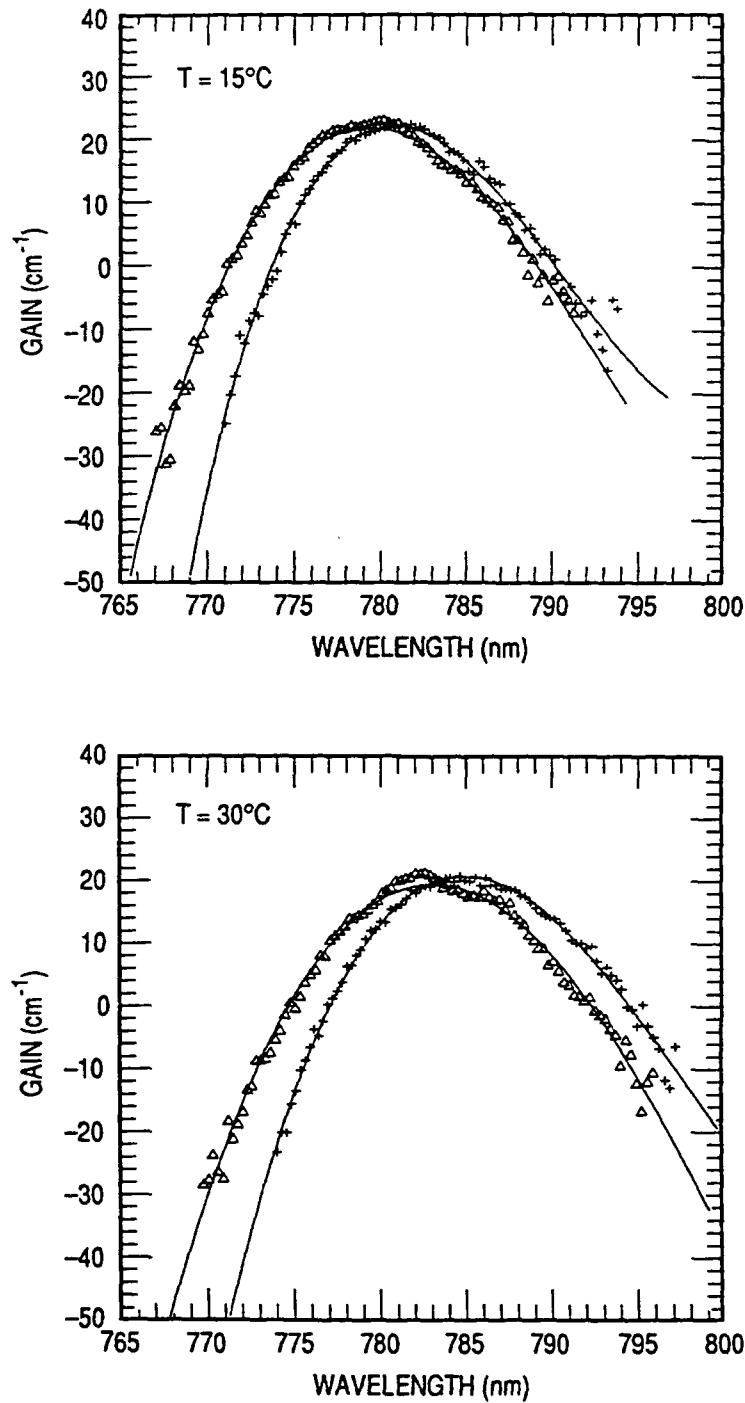
Figure 2. The blue shift of one of the model 4102-01 diode laser gain curves (laser 4A). Crosses correspond to the preirradiation gain curves. Triangles correspond to the gain curves after exposure to a fluence of 3×10^{13} n/cm^2. The solid lines are least-squares fits of the data to a fifth-order polynomial, which is used to find the energy of the gain curve peak E_p, and the energy where the gain is zero on the short-wavelength side of the gain curve ΔF_{cv}. Neutron exposure has led to a shift of the entire gain curve to shorter wavelengths.

Using the standard rate equation model describing laser dynamics,[24] one can show that the peak gain g of a semiconductor laser is linearly related to normalized injection current I/I_{th}:

$$g = (I/I_{th})(g_0 + \alpha_p/\Gamma) - g_0 \qquad (4)$$

Here α_p is the loss term for photons (including facet transmission and the photoionization of traps), Γ is the cavity filling factor, and g_0 is a term proportional to the minority carrier density required for transparency. It is to be noted that the peak gain in Eq. (5) does not depend explicitly on the rate of nonradiative recombination at recombination centers, which is known to increase following neutron irradiation.[13-15] Figure 3 illustrates the dependence of g on I/I_{th} at various levels of neutron exposure for laser 4A (all lasers showed similar behavior). Though laser 4A showed both an increase in its threshold current and a blue shift, the peak gain's dependence on I/I_{th} was unaffected. Consequently, the data of Fig. 3 suggest that neither α_p nor g_0 is significantly affected by fast neutrons up to 3×10^{13} n/cm^2. We note parenthetically that in fitting the g vs I/I_{th} curves to Eq. (5), all lasers showed nearly the same value of α_p (about 30 cm^{-1}); however, the 4102-01 diode lasers exhibited values of g_0 that were roughly three times larger than the g_0 values obtained for the 3101 diode lasers.

E_p is plotted as a function of I/I_{th} for lasers 4A and 3A at various levels of neutron exposure in Fig. 4. In general, all 4102-01 diode lasers displayed blue shifts of their gain curves by several meV following exposure to a neutron fluence of 2×10^{12} n/cm^2, while the 3101 diode lasers did not show a blue shift up to 3×10^{13} n/cm^2. Note that the blue shift persists to very low levels of normalized injection current, and that the magnitude of the blue shift is not very sensitive to normalized injection current. Together, these observations suggest that the mechanism giving rise to the blue shift is unrelated to minority-carrier scattering. If the blue shift mechanism were related to a nonlinear effect of minority-carrier scattering, then one would expect to see a small blue shift at low values of I/I_{th} and a larger shift at high values of I/I_{th}. Similar increases in ΔF_{cv} were obtained for the 4102-01 lasers, while the 3101 diode lasers showed no change in ΔF_{cv} . Since the magnitude of peak gain as a function of I/I_{th} is unaffected by fast neutrons, the ΔF_{cv} results would suggest that in order to achieve the same level of gain in the 4102-01 diode lasers following neutron irradiation, it is necessary to fill their bands to a higher level.

After burn-in, neither the 4102-01 nor the 3101 diode lasers showed any change in their dispersion curves up to 3×10^{13} n/cm^2. However, prior to burn-in and after an exposure of 2×10^{12} n/cm^2, all 4102-01 diode lasers showed an anomalous feature in their dispersion curves at a wavelength between 775 and 780 nm. This is illustrated in Fig. 5 for lasers 4A and 4B. The feature was not observed in the 3101 diode lasers, nor was it observed in the 4102-01 diode lasers after burn-in. (The small oscillation on the dispersion curves represents a 0.02 nm variation in the estimated cavity mode spacings, and is believed to be associated with a nonuniform drive rate of our monochromator grating.)
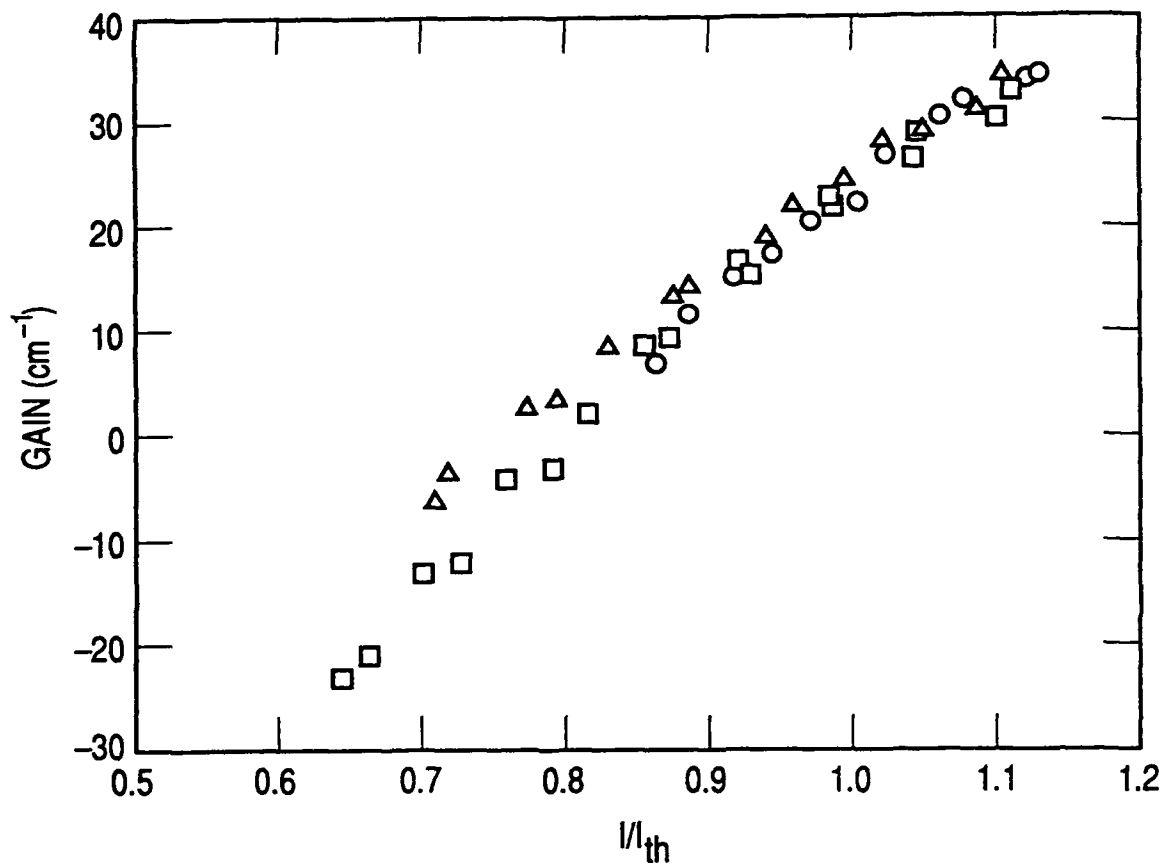
Figure 3. Peak gain vs I/I_{th} for laser 4A. Circles correspond to preirradiation results at both temperatures; squares correspond to both temperatures after 1×10^{13} n/cm^2; and triangles correspond to both temperatures after 3×10^{13} n/cm^2. Though this laser showed both an increase in its threshold current and a blue shift of its gain curve, the figure demonstrates that the relationship between gain and normalized injection current was unaffected by neutron exposure. This result is consistent with a mechanism in which fast neutrons increase the density of nonradiative recombination centers in the active region.
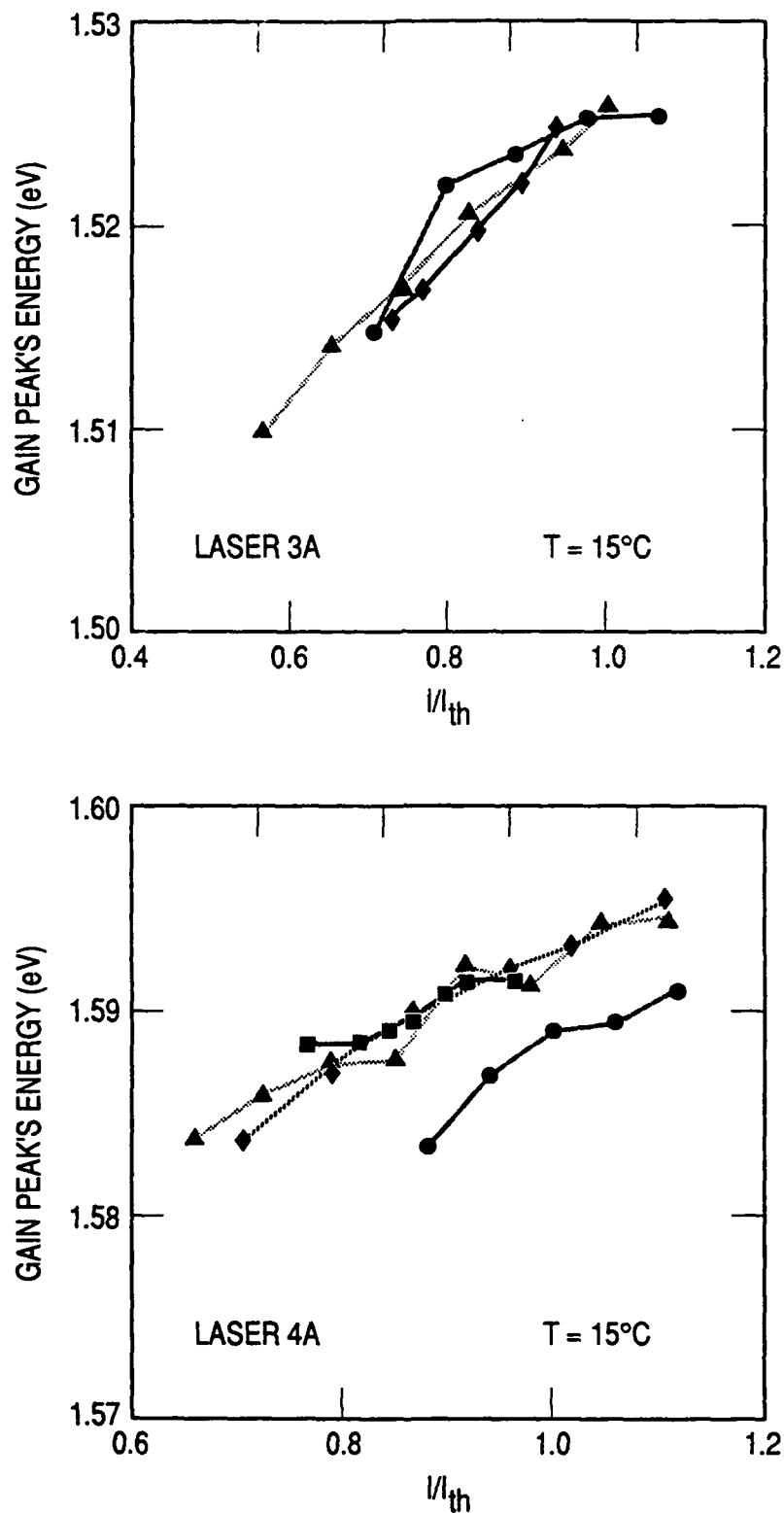
Figure 4. Energy of gain curve peak vs I/I_{th} for lasers 4A and 3A. Circles correspond to preirradiation results,; squares correspond to results following a neutron exposure of 2×10^{12} n/cm^2, and diamonds correspond to $3 \times 10^{12} n/cm^2$. Following exposure to a fast neutron fluence of $2 \times 10^{12} n/cm^2$, laser 4A shows a blue shift of E_p amounting to ~ 4 meV; at higher levels of exposure, this blue shift does not change. Laser 3A does not show such a shift.

16
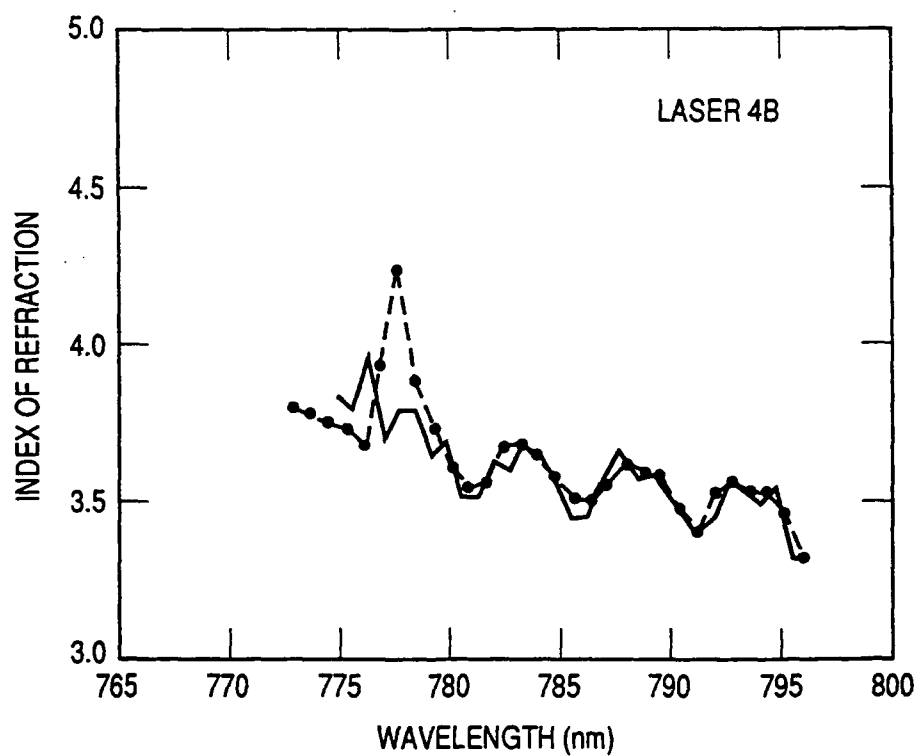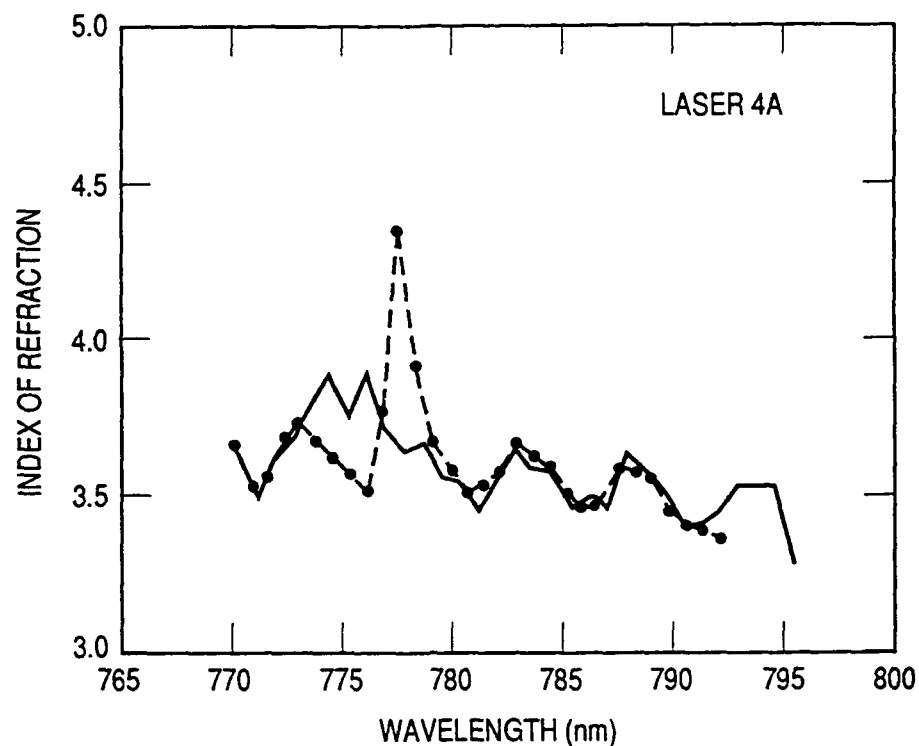
Figure 5. The solid lines are the lasers' dispersion curves prior to irradiation, while the circles correspond to dispersion curves after exposure to $2 \times 10^{12} n/cm^2$, but prior to burn-in. Following irradiation, there is a large change in the material's index of refraction between 775 and 780 nm. After burn-in, this feature was not observed. The oscillations in the data are believed to be due to a nonlinearity in the drive of our monochromator grating.

17

IV. POSSIBLE BLUE SHIFT MECHANISMS

As mentioned previously, neutron damage increases the attenuation coefficient for photons with energy less than E_g,[9] and this is possibly due to absorption by metallic-like zones ~10 nm in size.[5] This absorption would tend to depress the low-energy portion of the gain curve, and the resulting deformation could cause the gain curve peak to occur at higher energies, giving rise to a blue shift. However, this increase in the attenuation coefficient has only been observed after exposure to neutron fluences in excess of 10^{15} n/cm^2, whereas the blue shift in our experiments was observed at neutron fluence levels 3 orders of magnitude smaller than this. Moreover, one cannot ascribe the blue shift to a change in some higher-order absorption process, since the same magnitude shift was observed in both the linear and nonlinear regimes of field-matter interactions.

In addition to the increase in the attenuation coefficient, it is also well known that irradiation increases diode laser threshold current, an effect which is due to an increase in the rate of nonradiative recombination in the laser's active region. The energy that is released by the nonradiative recombination process appears in the form of heat, and this raises the temperature of the active region. However, since the band gap in AlGaAs is a decreasing function of temperature,[25] the most natural consequence of an increased rate of nonradiative recombination would be a red shift of the laser's gain curve.

Besides recombination centers, trapping states have been observed in GaAs following fast neutron irradiation.[10] Concerning laser operation, Bourkoff and Liu have shown that the presence of traps in the active region can increase the minority-carrier density.[26] Essentially, this effect arises because the traps can be photoionized, and this ionization acts as an additional source of minority carriers. The increased carrier density ΔN scales like $\sigma_T[T]$, where σ_T is the trap state ionization cross section and $[T]$ is the density of trapping states. For the case of electrons as the minority carrier, the increased carrier density would shift the conduction-band quasi-Fermi level to higher energies, and the resulting blue shift of the gain curve would be akin to a Burstein-Moss shift.[18] However, at the levels of neutron exposure under consideration ,the density of trapping states is expected to be an increasing function of neutron fluence, and therefore it is difficult to explain the saturation of the blue shift with this mechanism. Furthermore, since photoionization acts as a loss mechanism for photons, one would have expected to see a change in the dependence of peak gain on I/I_{th}.

Considering the band-gap energy of AlGaAs and its dependence on various parameters, it is worth noting that the band gap is an increasing function of hydrostatic pressure.[25] Since it is quite reasonable to expect neutron damage to increase the amount of stress in the laser's active region, one could expect this neutron-induced stress to increase the band-gap energy. Tuomi and Tiainen, in fact, used this mechanism to explain blue shifts of GaAs electroreflectance peaks following fast neutron irradiation, and estimated an equivalent hydrostatic pressure increase of 1.8 kbar for a neutron fluence of 10^{17} n/cm^2.[27] Assuming that this crystal stress is linear with neutron fluence, and not much different in AlGaAs, we would estimate an equivalent hydrostatic pressure increase of 0.18 bar for our neutron fluence of 10^{13} n/cm^2. Since the pressure coefficient of AlGaAs's band gap is ~ 11 µeV/bar,[25] this mechanism could only account for a ~ 2 µeV blue shift of the laser gain curves. This is to be compared with the several meV observed blue shifts.

19

One last candidate for the blue shift mechanism concerns the influence of irradiation on bandtail states. In order to obtain lateral waveguiding in a TJS diode laser, the device is subjected to a controlled Zn diffusion during fabrication. Consequently, the highly doped n-AlGaAs:Te active region ([Te] ~10^{18} cm^{-3}) is compensated with acceptors ([Zn] ~10^{19} cm^{-3})[28] and this can be expected to give rise to bandtailing.[29] Measurements of spontaneous emission in these devices have in fact found lasing photon energies 58 meV below the intrinsic band-gap energy,[30] indicating the participation of bandtail states in the lasing process. If neutron damage reduced the ability of these bandtail states to lase (i.e., "poisoned" them), lasing would be forced to take place between states of higher energy. The bandtail state poisoning would thus give rise to a blue shift of the gain curve.

Though one can imagine many processes that could lead to bandtail state poisoning (we will discuss one process subsequently), the general concept of bandtail state poisoning has several notable features. First, it provides an explanation of the blue shift that is independent of minority-carrier scattering and the regime of field-matter interactions. Consequently, it explains the blue shift in laser operation both above and below threshold. Further, since bandtail state poisoning does not necessarily affect the photon loss coefficient, a blue shift can be obtained without a change in the dependence of peak gain on I/I_{th}. Finally, if neutrons only poison the bandtail states, then the blue shift will saturate once the neutron fluence reaches a level where this poisoning is complete, even though the density of defects in the active region may still be an increasing function of neutron fluence at this level.

One possible process of bandtail state poisoning in compensated semiconductor material has been discussed by Arnold,[31] and requires that donor-to-acceptor transitions be responsible for lasing prior to neutron irradiation. The donor D and acceptor A form an ion pair, separated by some distance r, and the photon energy associated with the transition is given by[18]

$$E_{photon} = E_g - E_d - E_a + e^2 / \varepsilon r, \qquad (5)$$

where E_d (E_a) is the D (A) ionization energy, and ε is the dielectric constant of the material. For very distant pairs the photon energy will be relatively low, equal to $E_g - (E_d + E_a)$, while for the closest pairs the photon energy will be increased by the Coulomb attraction between the ions, $e^2/\varepsilon r$. As mentioned previously, fast neutrons create large regions of damage, and if a member of an ion pair should happen to be in one of these damaged regions, or even if a damaged region should happen to be present between the ions, it is reasonable to expect a poisoning of the D-A transition. Clearly, ion pairs with large r would be very sensitive to radiation damage, and would be poisoned at lower neutron fluence levels than ion pairs with small r. In this scheme, neutron exposure allows the ion pairs with a small spatial separation to dominate the lasing process, and this in turn results in a blue shift of the lasing transition. Saturation of the blue shift occurs when the gain associated with the D-A transitions becomes negligible compared with other transitions. Polimadei et al.[32] have employed this mechanism in an explanation of ~ 10 meV blue shifts observed in the luminescence peaks of AlGaAs light-emitting diodes (LEDs) following fast neutron irradiation. It should be mentioned though that the results of Polimadei et al. only dealt with the luminescence peak wavelength and not the entire luminescence spectrum, and furthermore only corresponded to a single neutron fluence level.

V. SEMIQUANTITATIVE MODEL OF THE BANDTAIL STATE POISONING EFFECT

In this section we demonstrate that a simple model of bandtail state poisoning explains many of our experimental observations. For the sake of clarity and simplicity, we will assume that lasing takes place between parabolic bands, and that k-selection rules are valid. Specific AlGaAs parameters are drawn from the review article by Adachi,[25] assuming a 0.1 mole fraction of aluminum. The bottom of the conduction band will represent the bandtail states, and their only distinction will be that they possess a conduction-to-valence-band matrix element that is sensitive to fast neutrons.

Below threshold the expression for diode laser gain is relatively straightforward to obtain, since it is simply related to the net rate of stimulated emission between the conduction and valence bands,[33,34]

$$g(E) = \kappa \int |M|^2 \rho_{red}(E)(f_c - f_v)L(E_{cv} - E)dE_{cv} \ . \tag{6}$$

Here, κ is a constant equal to $(e^2 h / 2\varepsilon_0 ncm_o^2 E)$; M is the matrix element coupling the conduction band to the valence band; ρ_{red} is the density of optical transitions at the energy E, *assuming k-selection rules*; f_c (f_v) is the electron occupation probability in the conduction (valence) band at energy E_c (E_v); and the integral is with respect to all energy separations E_{cv} between the conduction and valence band. The lineshape function $L(E_{cv} - E)$ accounts for phase damping of the dipole moment which is formed between the conduction and valence bands, and is typically assumed to have a Lorentzian character. The phase damping is an important characteristic of diode laser gain,[35] and a model incorporating phase damping as in Eq. (7) has been validated for TJS diode lasers.[36]

The Lorentzian function $L(E_{cv} - E)$ has a half-width $h/2\pi\tau_{in}$, where τ_{in} is the intraband scattering time which we set equal to 10^{-13} s.[36] The Lorentzian form for $L(E_{cv} - E)$, however, is not quite correct. The actual lineshape function falls off faster than a Lorentzian at values of $|E_{cv} - E| > 10h/2\pi\tau_{in}$,[37] and this may be an important consideration in the comparison of experimental gain curves with theory. Nonetheless, for convenience in our calculations we employed the Lorentzian line-shape function, truncating the Lorentzian at $|E_{cv} - E| = 10h/2\pi\tau_{in}$. Since we are not interested in a detailed comparison with experiment, this approximation is reasonable.

In order to model a poisoning of low-energy conduction-band states, we consider a situation in which the matrix element coupling the conduction and valence bands is a function of the conduction-band energy associated with the transition

$$|M|^2 + |M_0|^2 F(E_c) \ . \tag{7}$$

Here, M_0 is the matrix element prior to poisoning, assumed to be a constant independent of the transition energy, and $F(E_c)$ is a function describing the poisoning of conduction-band states. For simplicity we chose

$$F(E_c) = 1 - \exp\left[\left(E_g - E_c\right) / \left(E_{crit} - E_g\right)\right],$$ (8)

where E_{crit} is a parameter quantifying the degree of conduction-band poisoning. (The zero of energy in our calculations corresponds to the top of the valence band, and $E_g = 1.549$ eV.) For conduction-band energies E_c much less than E_{crit} we have $F(Ec) \sim 0$, and the poisoning is nearly complete. Alternatively, for conduction-band energies much greater than E_{crit} the matrix element is essentially unaffected by poisoning.

Results from a gain curve calculation including this form of conduction-band poisoning are shown in Fig. 6 ($p = 10^{19}$ cm^{-3}). The dashed curve corresponds to gain prior to irradiation $(E_{crit} = E_g)$, and it is readily apparent that E_p (unpoisoned) = 1.555 eV. The peak of the gain curve is therefore 6 meV above the band-gap energy employed in the calculations. When E_{crit} is set equal to $E_g + 6$ meV [i.e., E_p (unpoisoned)], the solid curve of Fig. 6 results. Clearly, this degree of conduction-band poisoning gives rise to a blue shift of the entire gain curve with the correct order of magnitude. For this same value of E_{crit}, Fig. 7 shows E_p as a function of gain. Since gain is unaffected by radiation, and is linearly proportional to I/I_{th}, this figure is equivalent to the experimental curves shown in Fig. 4. As was observed experimentally, the model predicts that the blue shift is nearly independent of normalized injection current, and persists to very low levels of normalized injection current.

It must be mentioned that in the calculation of the curves of Fig. 6, the conduction-band quasi-Fermi level is chosen so as to achieve a peak gain of 30 cm^{-1}. In the preirradiation case this requires a conduction-band electron concentration n of 1.6×10^{18} cm^{-3}. With $E_{crit} = E_g + 6$ meV, a peak gain of 30 cm^{-1} is achieved when $n = 1.7 \times 10^{18}$ cm^{-3}. If we let 30 cm^{-1} correspond to the laser's threshold gain, then the increase in n can be interpreted as a $\sim 10\%$ increase in the laser's threshold current. This neutron-induced increase in threshold current is distinct from the increase in threshold current that is required to compensate for an increased rate of nonradiative recombination as discussed by Barnes.[13-15] However, the actual amount of threshold current increase due to this poisoning effect should be a function of the density of-states' energy dependence in the poisoned band, and consequently it is difficult to estimate how large this effect should have been for our TJS lasers.

As illustrated in Fig. 8, a relatively large blue shift does not require that $E_{crit} = E_p$ (unpoisoned). In the figure, the magnitude of the blue shift is plotted as a function of $E_{crit} - E_g$. It is particularly noteworthy that for a value of E_{crit} that is 5 meV below E_p (unpoisoned), the magnitude of the blue shift is already nearly 1 meV. Consequently, to achieve an observable blue shift of the laser's gain curve, it is not necessary to poison those states with an energy equal to the gain curve's peak. An observable blue shift can result from the poisoning of states several meV below those originally identified with lasing.
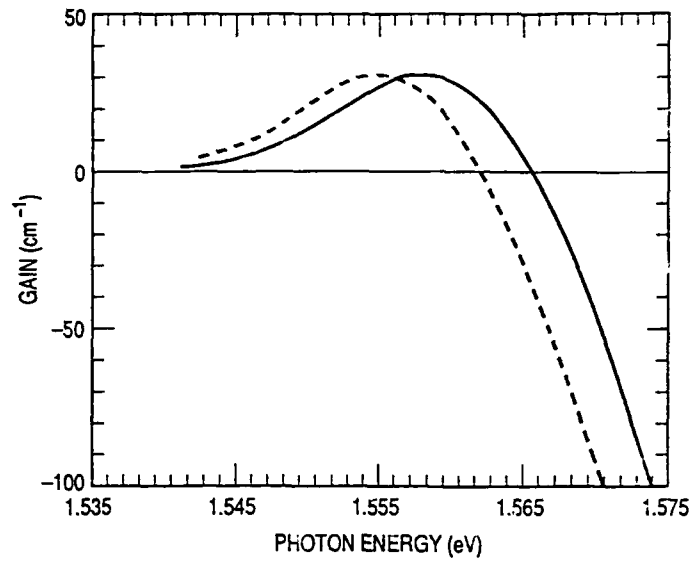
Figure 6. Model calculation of conduction-band poisoning due to neutron irradiation. The dashed curve corresponds to $(E_{crit} - E_g) = 0$, the preirradiated condition. The solid curve corresponds to $(E_{crit} - E_g) = 6$ meV, the postirradiated condition. It is clear that this mechanism for poisoning results in a ~ 3 meV blue shift of the entire gain curve.
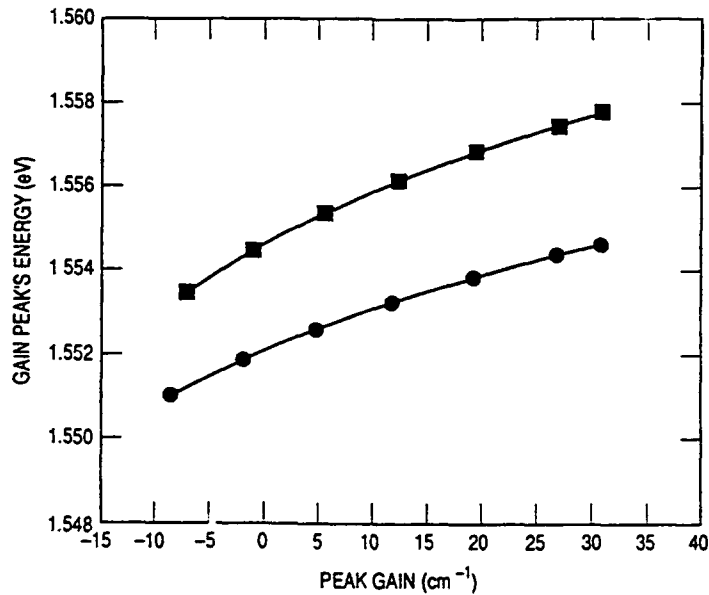

Figure 7. Energy of gain curve's peak vs gain. Circles correspond to unpoisoned (i.e., $E_{crit} = E_g$), while squares correspond to poisoned (i.e., $E_{crit} - E_g = 6$ meV). Since gain is linearly related to normalized injection current as demonstrated in Fig. 3, this figure illustrates the model's prediction for the dependence of E_p on I/I_{th}. The prediction is strikingly similar to the experimental curves shown in Fig. 4.
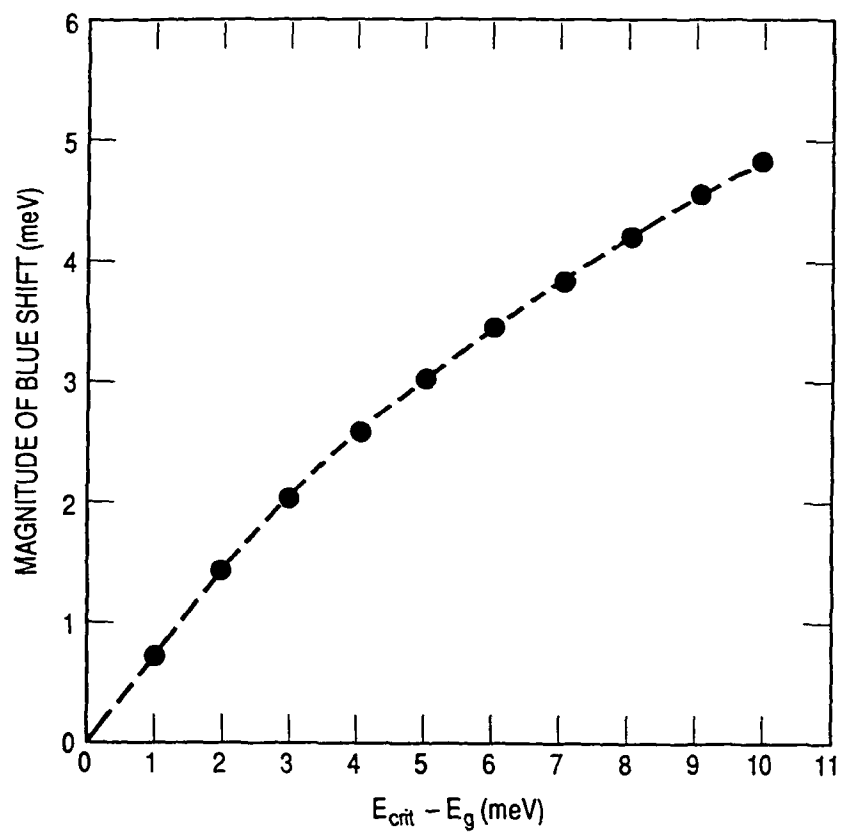
23

Figure 8. Magnitude of blue shift vs $E_{crit} - E_g$. Note that an observable blue shift does not require that poisoning be complete up to the levels originally identified with lasing. An observable blue shift of 1 meV can be obtained even if E_{crit} is 5 meV below the energy of these original conduction-band states

24

VI. DISCUSSION

In the present work we have found that in highly doped TJS diode lasers irradiation with fast neutrons can give rise to a blue shift of the laser's emission, and as discussed previously, we conjecture that this effect is associated with a poisoning of bandtail states for lasing. The most likely explanation for this bandtail state poisoning considers the lasing transition to be initially associated with a donor-to-acceptor impurity band transition. The introduction of damage regions into the semiconductor material following neutron irradiation poisons the low-energy D-A transitions, shifting the lasing transition to the blue. If this hypothesis is valid, then one could expect the magnitude of the blue shift to depend on both the level of doping in the material and the degree of compensation in the active region. Of course, there is still the question of why the blue shift seems to require burn-in before it is made manifest. As suggested by Moss[38] this may be related to a migration and fixing of traps next to impurities, in a manner akin to the $F_2^+(A)$ centers in the alkali halides.[39] At present, though, this is conjecture, and more work certainly needs to be done on the role of burn-in and the appearance of the blue shift in order to obtain definitive explanations.

Irrespective of the actual mechanism of the blue shift, we are nonetheless faced with the question of why the model 4102-01 diode lasers showed a blue shift, but the model 3101 diode lasers did not. It might be that the 3101 diode lasers do show the effect, but only after exposure to much higher fluence levels. This, however, begs the question of why the model 4102-01 diode lasers are then more sensitive to fast neutron irradiation. There is a difference in the Al content in the devices; the model 4102-01 diode lasers have more Al in their active regions, since their lasing wavelength is shorter. In this regard it is worth noting that in the work of Polimadei *et al.*[32], the blue shift of LED luminescence peaks was maximum (34 meV) for an Al mole fraction of 0.18. For mole fractions of Al less than 0.18, the blue shift was smaller. Our results are certainly consistent with these findings, since the 4102-01 diode lasers had an Al mole fraction of 0.13 and the 3101 diode lasers had an Al mole fraction of 0.08. However, why the blue shift magnitude should be sensitive to the mole fraction of Al is unclear. This question is especially puzzling given the fact that standard damage coefficients, which account for neutron induced increases in nonradiative recombination rates, are a monotonically decreasing function of Al content.[32,40]

REFERENCES

1. See, for example, J C. Camparo and R. P. Frueholz, I. Appl. Phys. 59, 3313 (1986); *Frequency Standards and Metrology,* edited by A. DeMarchi (Springer, Berlin, 1989), and references therein.

2. J. C. Camparo, in *Proceedings of the International Conference on Lasers '88,* edited by R. C. Sze and F. J. Duarte (STS, McLean, VA, 1989), pp. 546553.

3. L. W. Aukerman, P. W. Davis, R. D. Graft, and T. S. Shilliday, *J. Appl. Phys.* 34, 3590 (1963).

4. R. Coates and E. W. J. Mitchell, *Adv. Phys.* 24, 593 (1975).

5. J. L. McNichols and W. S. Ginell, *J Appl. Phys.* 38, 656 (1967).

6. T. O. Tuomi and O. J. A. Tiainen, *Phys. Rev. Lett.* 29, 1452 (1972).

7. P. J. Griffin, M. S. Lazo, T. F. Luera, and J. G. Kelly, *IEEE Trans. Nucl. Sci.* NS-36, 1937 (1989).

8. K. V. Vaidyanathan, L. A. K. Watt, and M. L. Swanson, *Phys. Status Solidi A* 10, 127 (1972).

9. V. C. Burkig, J. L. McNichols, and W. S. Ginell, *J. Appl. Phys.* 40, 3268 (1969); B. E. Kincaid, *Appl. Opt.* 25, 1736 (1986).

10. J. E. Ludman and W. B. Nowak, *Solid-State Electron.* 19, 759(1976).

11. V. F. Kovalenko, G. P. Peka, and 0. A. Tokalin, *Sov. Phys. Semicond.* 19 626 (1985).

12. V. A. Vilkotskii, D. S. Domanevskii, V. M. Lomako, and V. D. Tkachev, *Sov. Phys. Semicond.* 7, 249 (1973).

13. C. E. Barnes, *J. Appl. Phys.* 42, 1941 (1971); 45, 3485 (1974).

14. C. E. Barnes, in *Laser and Laser Systems Reliability* (SPIE, Bellingham, WA, 1982), pp. 88-95.

15. C. E. Barnes, *IEEE Trans. Nucl. Sci.* NS-19, 382 (1972).

16. T. L. Paoli, *IEEE IJ Quantum Electron.* QE-11, 489 (1975).

17. B. W. Hakki and T. L. Paoli, *J. Appl. Phys.* 44, 4113 (1973); 46, 1299 (1975).

18. J. I. Pankove, *Optical Processes in Semiconductors* (Dover, New York, (1975).

19. H. C. Casey, Jr. and M. B. Panish, *Heterostructure Lasers* (Academic, New York, 1978), Part B, p. 16.

20. H. C. Casey, Jr., D. D. Sell, and M. B. Panish, *Appl. Phys. Lett.* **24**, 63 (1974)~

21. See, for example, R. J. Chaffin, *Microwave Semiconductor Devices: Fundamentals and Radiation Effects* (Wiley, New York, 1973), p. 376.

22. J. C. Camparo, Contemp. Phys. **26**, 443 (1985).

23. J. C. Camparo and C. H. Volk, *IEEE J Quantum Electron.* **QE-18**, 1990 (1982).

24. K. Y. Lau and A. Yariv, in *Semiconductors and Semimetals*, edited by W. T. Tsang (Academic, Orlando, FL, 1985), Vol. 22, Part B, pp. 69-152.

25. S. Adachi, *J Appl. Phys.* **58**, RI (1985).

26. E .Bourkoff and X. Y. Liu, *J. Appl. Phys.* **65**, 2912 (1989).

27. T. Tuomi and O. J A. Tiainen, *Surf. Sci.* **37**, 617 (1973).

28. W. Susaki, T. Tanaka, H. Kan, and M. Ishii, IEEE *J. Quantum Electron.* **QE-13**, 587 (1977).

29. Following Pankove (Ref. 18), bandtailing is taken as a very general term. Processes that would induce bandtailing in the present context could include impurity band formation as well as deformation potentials and Coulomb interactions.

30. H. Namizaki, H. Kumabe, and W. Susaki, *IEEE J. Quantum Electron.* **QE-17**, 799 (1981).

31. G. W. Arnold, Phys. Rev. **183**, 777 (1969).

32. R. A. Polimadei, S. Share, A. S. Epstein, R. J. Lynch, and D. Sullivan, *IEEE Trans. Nucl. Sci.* **NS-21**, 96 (1974).

33. G. H. B. Thompson, *Physics of Semiconductor Laser Devices* (Wiley, Chichester, 1980).

34. R. H. Yan, S. W. Corzine, L. A. Coldren, and I. Suemune, *IEEE J. Quantum Electron.* **QE-26**, 213 (1990).

35. See, for example, M. Asada and Y. Suematsu, *IEEE J. Quantum Electron.* **QE-21**, 434 (1985), and references therein.

36. M. Yamada, A. Tanaka, K. Moriya, and Y. Kado, *Appl. Phys. Lett.* **43**, 818 (1983).

37. M. Yamanishi and Y. Lee, *IEEE J. Quantum Electron.* **QE-23**, 367 (1987).

38. S. C. Moss (private communication).

39. I. Schneider and M. J Marrone, *Opt. Lett.* **4**, 390 (1979).

40. A. P. Karatsyuba, M. V. Ovanesov, and V. P. Sushkov, Sov. Phys. Semicond. **14**, 862 (1980).